https://doi.org/10.1007/s11467-022-1229-3

RESEARCH ARTICLE

Deterministic and replaceable transfer of silver flakes for microcavities

Tingting Wang[1,2], Zhihao Zang[1], Yuchen Gao[1], Kenji Watanabe[3], Takashi Taniguchi[4], Wei Bao[5],Yu Ye[1,2,6,†]

[1] State Key Laboratory for Mesoscopic Physics and Frontiers Science Center for Nano-optoelectronics, School of Physics, Peking University, Beijing 100871, China
[2] Collaborative Innovation Center of Quantum Matter, Beijing 100871, China
[3] Research Center for Functional Materials, National Institute for Materials Science, 1-1 Namiki, Tsukuba, 305-0044, Japan
[4] International Center for Materials Nanoarchitectonics, National Institute for Materials Science, 1-1 Namiki, Tsukuba, 305-0044, Japan
[5] Electrical & Computer Engineering, University of Nebraska-Lincoln, Nebraska 68588, USA
[6] Yangtze Delta Institute of Optoelectronics, Peking University, Nantong 226010, China
Corresponding author. E-mail: [†]ye_yu@pku.edu.cn

Received October 7, 2022; accepted November 25, 2022

Supporting Information

S1. Optical image of continuous silver flakes

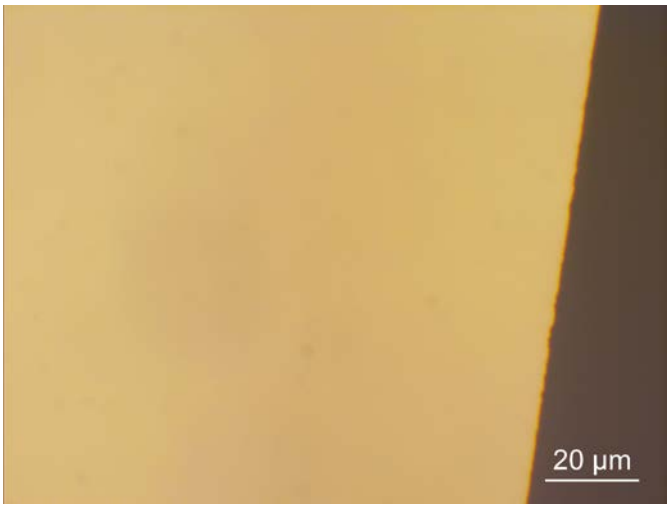

Fig. S1 Optical image of large-scale continuous silver flakes transferred on the polydimethylsiloxane (PDMS) substrate.

S2. Transferability of silver mirrors of different thicknesses

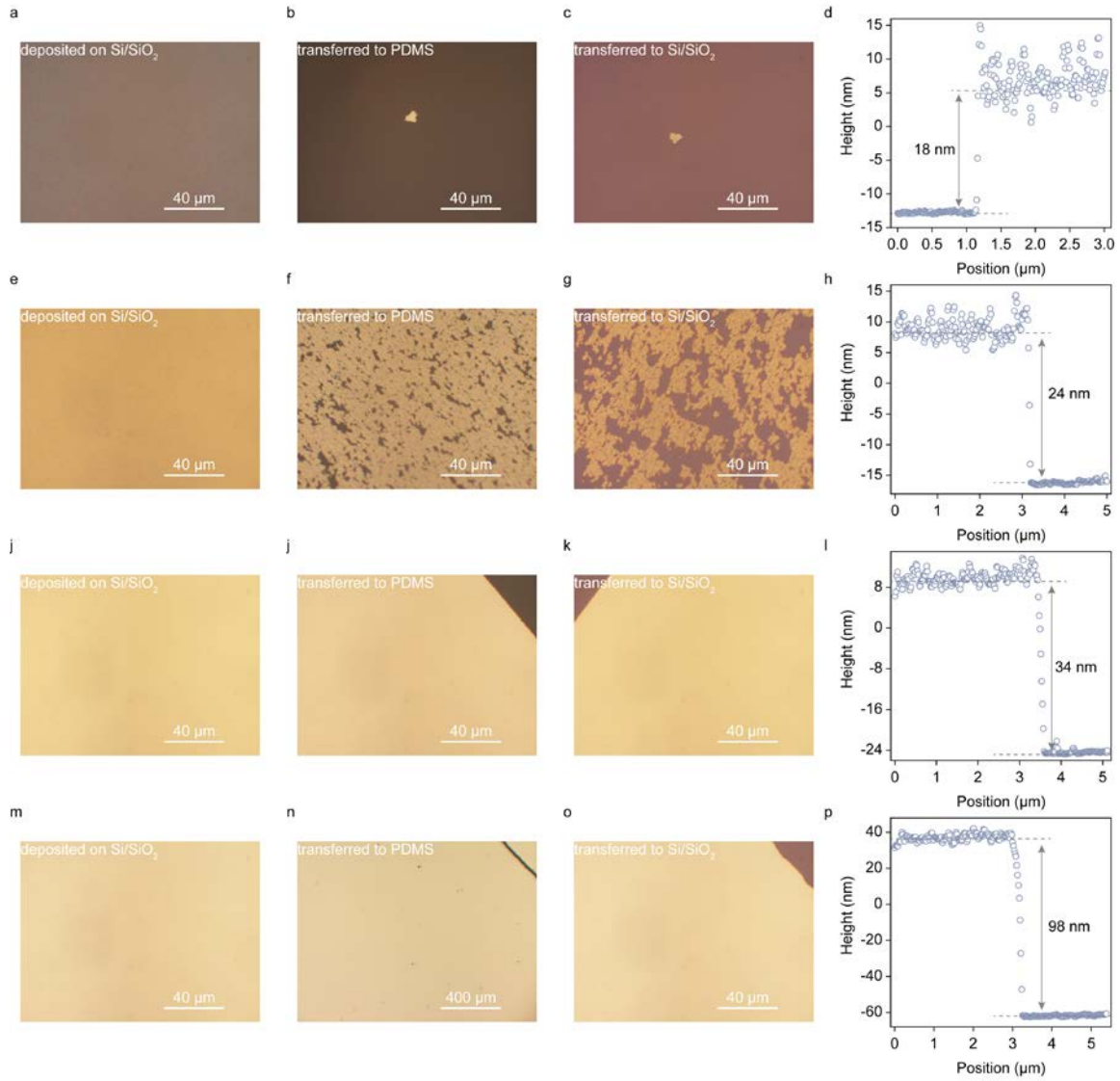

Fig. S2 Deterministic transfer and thickness characterization of silver flakes with different thicknesses. **(a-c, e-g, i-k, and m-o)** Optical microscope images of 18 nm, 24 nm, 34 nm and 98 nm thick silver films deposited on Si/SiO_2 substrates, transferred to PDMS substrates, and transferred to target Si/SiO_2 substrates, respectively. **(d, h, i, p)** The corresponding height line profiles of the transferred silver flakes on target Si/SiO_2 substrates.

S3. Deterministic transfer of gold flakes

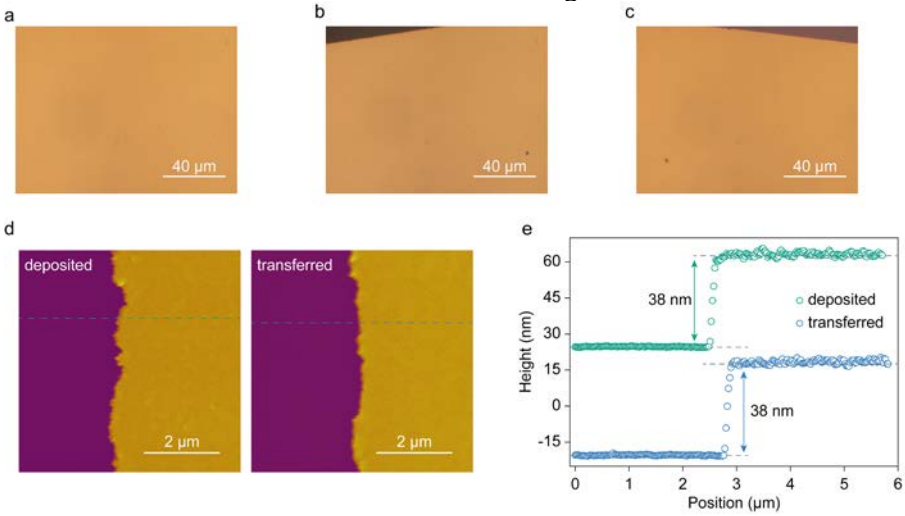

Fig. S3 Deterministic transfer and thickness characterization of gold flakes. **(a-c)** Optical microscope images of gold film deposited on Si/SiO_2 substrate (a), peeled off by PDMS substrate (b), and transferred onto another Si/SiO_2 substrate (c), respectively. **(d-e)** Atomic force microscope height images and the corresponding height line profiles (along the dashed lines marked in (d)) of the deposited and transferred gold flakes.

S4. Roughness characterization of silver flakes

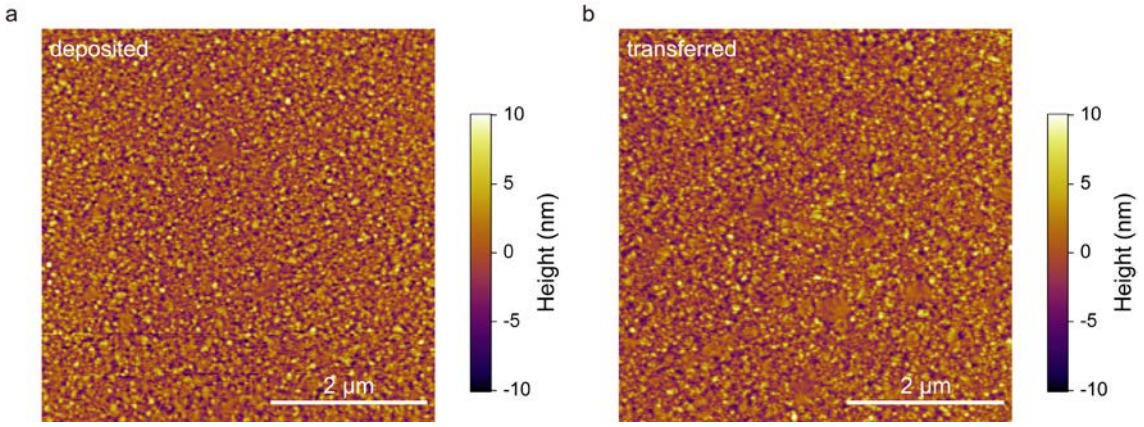

Fig. S4 Surface roughness characterizations of the deposited silver flake **(a)** and the transferred silver flake **(b)**. Within the area of 25.3 μm^2, the surface roughness of the silver flake deposited on the Si/SiO_2 substrate is R_a = 2.047 nm, while the surface roughness of the silver flake transferred to the Si/SiO_2 substrate is R_a = 1.975 nm.

Note S1. Dispersion fitting

Traditionally, strong coupling behavior can be described by a simplified coupled oscillator model that ignores linewidth:

$$\begin{bmatrix} E_c & V \\ V & E_{ex} \end{bmatrix} \begin{bmatrix} a \\ b \end{bmatrix} = E \begin{bmatrix} a \\ b \end{bmatrix}, \quad (1)$$

where E_c is the cavity mode (E_{ca} and E_{cb} correspond to cavity modes along the *a*- and *b*-axis, respectively), E_{ex} is the exciton energy, E is the eigenvalue corresponding to the polariton mode energy, a and b define the eigenvectors of the polariton modes, and V is the coupling strength between the exciton state and photonic mode. Owing to the multilayer structure of our device, we can derive the cavity mode as

$$E_c(\theta) = \frac{mhc}{\sum_i \frac{2n_i L_i}{\sqrt{1-\left(\frac{\sin\theta}{n_i}\right)^2}}}, \quad (2)$$

where m is the mode order, θ is the emission angle relative to the *z*-axis, n_i and L_i are the refractive index and thickness of the *i*th layer, respectively.

To avoid fitting errors, we obtain a series of material parameters from our experiments or references to reduce the number of free-tuning parameters. The cavity modes are calculated from the fixed thickness and refractive index of each layer in the cavity, while the exciton energies are directly extracted from their absorption spectra at different temperatures.

In this way, for the microcavity in Fig. 2(d), the degenerate exciton energy extracted from the room temperature absorption spectrum is 2.3574 eV, and the best fit yields a cavity mode of E_{ca} = 2.3176 eV along the *a*-axis and a cavity mode of E_{cb} = 2.3297 eV along the *b*-axis. In addition, we obtain the Rabi splitting energy, $\hbar\Omega$, between the lower polariton (LP) branch and the upper polariton (UP) branch along the *a*-axis and *b*-axis, which are 107.94 meV and 96.23 meV, respectively.

Similarly, for the microcavities in Figs. 3(h) and (i), the degenerate exciton energy is maintained at 2.3608 eV. As for the microcavity in Fig. 3(h), the best fit yields a cavity mode of 6 E_{ca} = 2.3978 eV along the *a*-axis and a cavity mode of E_{cb} = 2.4061 eV along the *b*-axis. In addition, we obtain the Rabi splitting energy, $\hbar\Omega$, between the LP branch and the UP branch along the *a*-axis and *b*-axis, which are 53.45 meV and 42.19 meV, respectively. After the subsequent transfer steps, for the microcavity in Fig. 3(i), the best fit yields a cavity mode of E_{ca} = 2.3561 eV along the *a*-axis and a cavity mode of E_{cb} = 2.3641 eV along the *b*-axis. In addition, we obtain the Rabi splitting energy, $\hbar\Omega$, between the LP branch and the UP branch along the *a*-axis and *b*-axis, which are 68.77 meV and 60.83 meV, respectively.

S5. Fitting of exciton-polariton emission

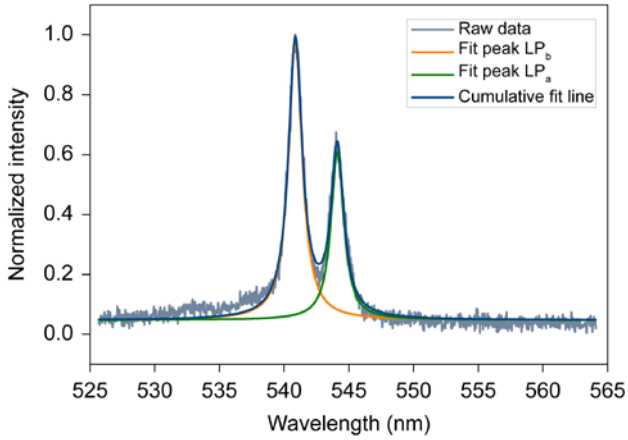

Fig. S5 Photoluminescence spectrum of exciton-polariton emission recorded at θ =0◦ (shadow blue line) and its corresponding fitting lines. The yellow, green and safety blue lines display the fittings of the LP dispersion LPb, LPa, and the cumulative peak, respectively. LPa (LPb) is centered at 544.1 nm (540.9 nm) with an full width at half maximum of 1.20 nm (1.29 nm), corresponding to a quality factor of ∼454 (∼420).

S6. Optical image of the top h-BN layer on PDMS substrate

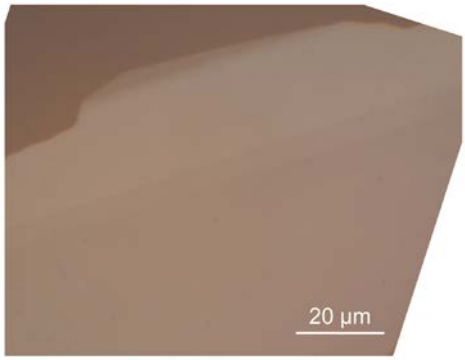

Fig. S6 The optical image of the h-BN layer exfoliated on PDMS substrate, which helps outline its profile in the optical image of the device in Fig. 3(f) in the main text.

S7. Hopfield coefficients

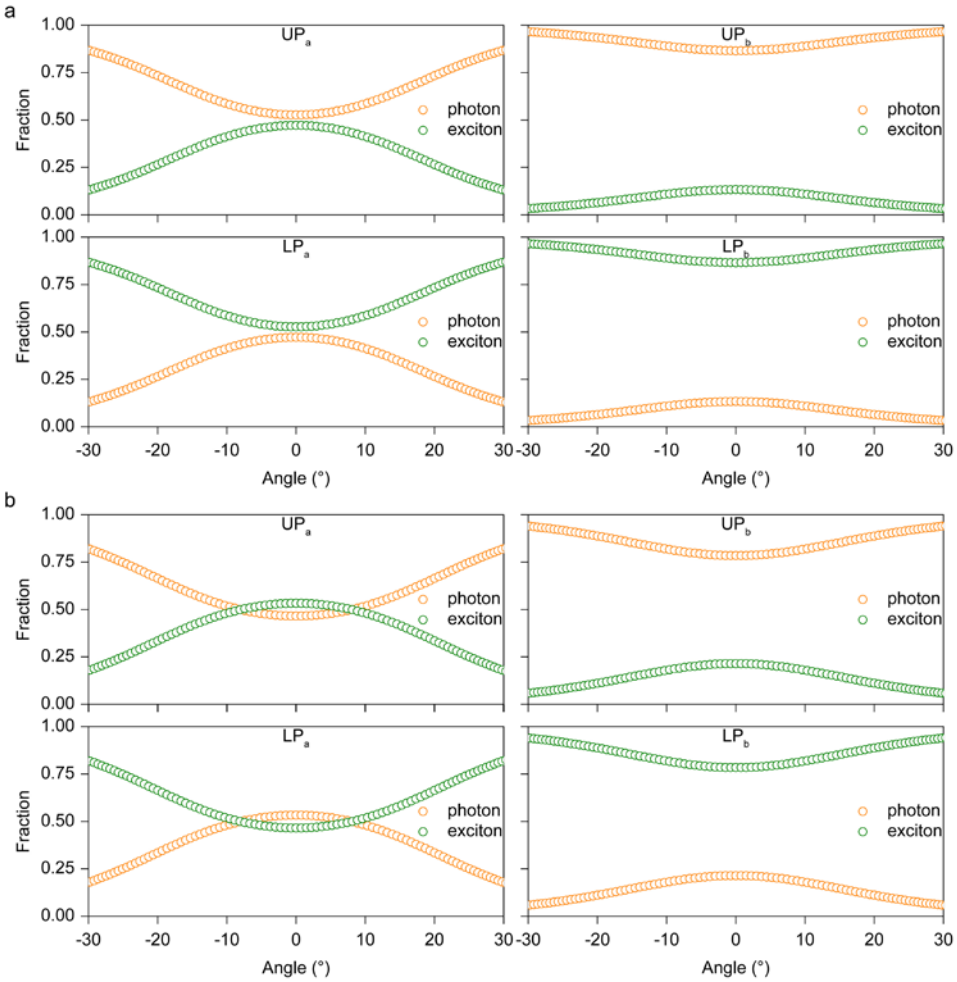

Fig. S7 Fitted Hopfield coefficients. **(a, b)** Fitted Hopfield coefficients of the cavity photons and excitons for the polariton branches with polarizations along the *a*-axis and *b*-axis in Fig. 3(h) (a) and Fig. 3(i) (b) in the main text.